

## $J/\psi$ Production in Quark-Gluon Plasma

Li Yan,<sup>1</sup> Pengfei Zhuang,<sup>1</sup> and Nu Xu<sup>2</sup>

<sup>1</sup>*Physics Department, Tsinghua University, Beijing 100084, China*

<sup>2</sup>*Nuclear Science Division, Lawrence Berkeley National Laboratory, Berkeley, California 94720, USA*

(Received 2 August 2006; published 4 December 2006)

We study  $J/\psi$  production at RHIC and LHC energies with both initial production at energies reached and the BNL Relativistic Heavy Ion Collider (RHIC) and CERN Large Hadron Collider (LHC) with regeneration. We solve the coupled set of transport equations for the  $J/\psi$  distribution in phase space and the hydrodynamic equation for evolution of quark-gluon plasma. At RHIC, continuous regeneration is crucial for the  $J/\psi$  momentum distribution while the elliptic flow is still dominated by initial production. At energies reached at the LHC energy, almost all the initially created  $J/\psi$ s are dissociated in the medium and regeneration dominates the  $J/\psi$  properties.

DOI: [10.1103/PhysRevLett.97.232301](https://doi.org/10.1103/PhysRevLett.97.232301)

PACS numbers: 25.75.Dw, 12.38.Mh, 24.85.+p

The goal of high-energy nuclear collisions is to identify and study the equation of state of the quark-gluon plasma (QGP) which is believed to exist at the early stage of our Universe [1]. In  $\sqrt{s_{NN}} = 200$  GeV Au + Au collisions, the observations of jet quenching [2] and collective flow have demonstrated the formation of hot and dense matter with partonic collectivity [3,4]. Local thermalization of the system created in heavy ion collisions is yet to be tested. Heavy flavors including charm and bottom quarks are powerful tools [5] for studying the early collision dynamics because their masses are much larger than possible excitation temperature, for example, of the system created in collisions at RHIC. Recent results have shown that heavy flavors are all produced in the initial collisions [6,7]. Therefore, studying open charm and charmonium production will yield important information on the properties of QGP. The  $J/\psi$  is a particularly sensitive probe of the early stages because its survival probability depends on the environment. Lattice gauge theory calculations have indicated that  $J/\psi$ s do exist above the critical temperature [8,9].

The  $J/\psi$  suppression was first proposed as a direct signature to identify the QGP formation 20 years ago [10]. Besides the normal suppression induced by nuclear absorption, the  $J/\psi$ s initially produced by hard processes are anomalously suppressed [11–17] by interactions in the hot medium. While charm quark production at the SPS is expected to be small, there are more than 10  $c\bar{c}$  pairs produced in a central Au + Au collision at RHIC, and is probably more than 200 pairs at the LHC [18]. These uncorrelated charm quark pairs in the QGP can be recombined to form  $J/\psi$ s. Obviously, regeneration will enhance the  $J/\psi$  yield and alter its momentum spectra. Recently, the regeneration approach for  $J/\psi$  production at RHIC has been widely discussed with different models, such as thermal production on the hadronization hypersurface according to statistic law [19–21], the coalescence mechanism [22], and the kinetic model [23,24] which considers continuous  $J/\psi$  regeneration in a QGP.

The medium created in high-energy nuclear collisions evolves dynamically. In order to extract information about the medium by analyzing the  $J/\psi$  distributions, both the hot and dense medium and the  $J/\psi$  production processes must be treated dynamically. In this Letter, we treat continuous regeneration of the  $J/\psi$  in a QGP self-consistently, including hydrodynamic evolution of the QGP itself. Both regenerated and initially produced  $J/\psi$ s are simultaneously taken into account. Including both processes is important for RHIC since, unlike the collisions at the LHC, not all the initially produced  $J/\psi$ s are destroyed.

The massive  $J/\psi$ s are unlikely fully thermalized with the medium. Thus their phase space distribution should be governed by transport rather than the kinetic equation of Refs. [23,24]. To comprehensively treat the  $J/\psi$  distribution, we determine the  $J/\psi$  transport equation including both initial production and anomalous suppression as well as regeneration. The transport equation is then solved together with the hydrodynamic equation which characterizes the space-time evolution of the QGP. In order to compare with the experimental measurements, we calculate the average transverse momentum squared  $\langle p_t^2 \rangle$ , elliptic flow  $v_2$ , and nuclear modification factor  $R_{AA}$ , for  $J/\psi$  at both RHIC and LHC.

In  $p + p$  collisions, about 30%–40% of final state  $J/\psi$ s are from the feed-down [25] of  $\psi'$  and  $\chi_c$ . In order to simplify the numerical calculation, we neglect the  $\psi'$  contribution and assume 40% of the final state  $J/\psi$ s come from  $\chi_c$  [16]. Since the  $\Psi (= J/\psi, \chi_c)$  is heavy, we use a classical Boltzmann-type transport equation to describe its evolution. The distribution function  $f_{\Psi}(\mathbf{p}_t, \mathbf{x}_t, \tau|\mathbf{b})$  in the central rapidity region and in the transverse phase space  $(\mathbf{p}_t, \mathbf{x}_t)$  at fixed impact parameter  $\mathbf{b}$  is controlled by the equation

$$\partial f_{\Psi}/\partial\tau + \mathbf{v}_{\Psi} \cdot \nabla f_{\Psi} = -\alpha_{\Psi} f_{\Psi} + \beta_{\Psi}. \quad (1)$$

The second term on the left-hand side arises from free streaming of  $\Psi$  with transverse velocity  $\mathbf{v}_{\Psi} = \mathbf{p}_t/\sqrt{\mathbf{p}_t^2 + m_{\Psi}^2}$ , which leads to the “leakage” effect and

is needed to explain the averaged transverse momentum squared at the SPS [15]. The anomalous suppression and regeneration mechanisms are reflected in the loss term  $\alpha_\Psi$  and gain term  $\beta_\Psi$ , respectively.

Suppose the medium locally equilibrates at time  $\tau_0$ , when nuclear absorption of the initially produced  $J/\psi$ s has ceased. Absorption effects can be included in the initial distribution [15,16],  $f_\Psi(\mathbf{p}_t, \mathbf{x}_t, \tau_0|\mathbf{b})$ , of the transport equation.

$$f_\Psi(\mathbf{p}_t, \mathbf{x}_t, \tau|\mathbf{b}) = f_\Psi(\mathbf{p}_t, \mathbf{x}_t - \mathbf{v}_\Psi(\tau - \tau_0), \tau_0|\mathbf{b})e^{-\int_{\tau_0}^{\tau} d\tau' \alpha_\Psi(\mathbf{p}_t, \mathbf{x}_t - \mathbf{v}_\Psi(\tau - \tau'), \tau'|\mathbf{b})} + \int_{\tau_0}^{\tau} d\tau' \beta_\Psi(\mathbf{p}_t, \mathbf{x}_t - \mathbf{v}_\Psi(\tau - \tau'), \tau'|\mathbf{b})e^{-\int_{\tau'}^{\tau} d\tau'' \alpha_\Psi(\mathbf{p}_t, \mathbf{x}_t - \mathbf{v}_\Psi(\tau - \tau''), \tau''|\mathbf{b})}. \quad (2)$$

The first and second terms on the right-hand side indicate the contributions from the initial production and continuous regeneration, respectively. Both suffer anomalous suppression. The coordinate shift  $\mathbf{x}_t \rightarrow \mathbf{x}_t - \mathbf{v}_\Psi \Delta\tau$  reflects the leakage effect during the time period  $\Delta\tau$ .

We determine now the  $J/\psi$  suppression and regeneration in a QGP. We consider only the gluon dissociation process,  $g + \Psi \rightarrow c + \bar{c}$ , for the loss term [16]. Its inverse process is the gain term. Then  $\alpha_\Psi$  and  $\beta_\Psi$  are

$$\alpha_\Psi(\mathbf{p}_t, \mathbf{x}_t, \tau|\mathbf{b}) = \frac{1}{2E_\Psi} \int \frac{d^3\mathbf{p}_g}{(2\pi)^3 2E_g} W_{g\Psi}^{c\bar{c}}(s) f_g(\mathbf{p}_g, \mathbf{x}_t, \tau) \Theta(T(\mathbf{x}_t, \tau|\mathbf{b}) - T_c),$$

$$\beta_\Psi(\mathbf{p}_t, \mathbf{x}_t, \tau|\mathbf{b}) = \frac{1}{2E_\Psi} \int \frac{d^3\mathbf{p}_g}{(2\pi)^3 2E_g} \frac{d^3\mathbf{p}_c}{(2\pi)^3 2E_c} \frac{d^3\mathbf{p}_{\bar{c}}}{(2\pi)^3 2E_{\bar{c}}} \times W_{c\bar{c}}^{g\Psi}(s) f_c(\mathbf{p}_c, \mathbf{x}_t, \tau|\mathbf{b}) f_{\bar{c}}(\mathbf{p}_{\bar{c}}, \mathbf{x}_t, \tau|\mathbf{b}) (2\pi)^4 \delta^{(4)}(p + p_g - p_c - p_{\bar{c}}) \Theta(T(\mathbf{x}_t, \tau|\mathbf{b}) - T_c), \quad (3)$$

where  $E_g$ ,  $E_\Psi$ ,  $E_c$  and  $E_{\bar{c}}$  are the gluon, charmonium,  $c$ , and  $\bar{c}$  energies. The step function  $\Theta$  ensures that anomalous suppression and regeneration occur only in the QGP phase. The gluon thermal distribution is  $f_g$ .  $W_{g\Psi}^{c\bar{c}}(s)$  [28] is transition probability of the gluon dissociation as a function of  $s = (p + p_g)^2$  calculated in pQCD [28], and  $W_{c\bar{c}}^{g\Psi}$  is  $c$  and  $\bar{c}$  recombination transition probability. Note that  $W_{c\bar{c}}^{g\Psi}$  can be obtained from  $W_{g\Psi}^{c\bar{c}}$  using detailed balance. In numerical calculations, we take  $m_c = 1.87$  GeV, including in-medium effects [16,23],  $m_{J/\Psi} = 3.1$  GeV,  $m_{\chi_c} = 3.51$  GeV, and critical temperature  $T_c = 165$  MeV.

Unlike gluons that are constituents of a QGP, charm quarks are heavy and may not be thermalized in the QGP. In principle, a self-consistent treatment of charm quark motion in the QGP should be described by a transport equation similar to Eq. (1). For simplicity, we consider the  $c$  and  $\bar{c}$  distribution functions,  $f_c$  and  $f_{\bar{c}}$ , in two extreme scenarios. In the weak interaction limit, the charm quarks in QGP are assumed to keep their original momentum distribution,  $g_c(\mathbf{q})$ , calculated in pQCD [24] and their initial space distribution determined by nuclear geometry,

$$f_{c,\bar{c}}(\mathbf{q}, \mathbf{x}_t|\mathbf{b}) = \sigma_{pp}^{c\bar{c}} T_A(\mathbf{x}_t) T_B(\mathbf{x}_t - \mathbf{b}) g_c(\mathbf{q}), \quad (4)$$

where  $\sigma_{pp}^{c\bar{c}} = 622 \pm 57 \mu\text{b}$  [29] is the charm production cross section at RHIC. In the opposite limit, when the  $c$  and  $\bar{c}$  are strongly correlated to the medium, they are thermalized and distributed statistically. Both the pQCD and ther-

mal distributions are normalized to the initial charm quark number. To determine the initial condition at RHIC, we take  $\tau_0 = 0.6$  fm, the initial  $J/\psi$  production cross section  $\sigma_{pp}^\Psi = 2.61 \pm 0.20 \mu\text{b}$  [26] and nuclear absorption cross section  $\sigma_{\text{abs}} = 3$  mb [27]. We also assume that  $a_{gN} = 0.076$  GeV<sup>2</sup>/fm and  $\langle p_t^2 \rangle_{pp} = 4.31$  GeV<sup>2</sup> [26] to describe the initial  $p_t$  broadening due to multiple gluon scattering.

When the loss and gain terms  $\alpha_\Psi$  and  $\beta_\Psi$  are known, the transport Eq. (1) can be solved analytically with the result

mal distributions are normalized to the initial charm quark number.

Since the hadronic phase occurs later in the evolution of heavy ion collisions when the density of the system is lower compared to the early hot and dense period, we have neglected the hadronic dissociation. The suppression and regeneration region controlled by the step function in the loss and gain terms and the gluon and thermal charm quark distributions are determined by the QGP evolution. With the Hubble-like longitudinal expansion and boost invariant initial condition, the transverse hydrodynamical equations [16] can be solved numerically to determine the evolution of temperature and transverse fluid velocity.

The final state  $J/\psi$  distributions at fixed centrality can be found by integrating the distribution function, Eq. (2), over  $\mathbf{p}_t$  and  $\mathbf{x}_t$  up to  $\tau \rightarrow \infty$ . We first examine the mid-rapidity nuclear modification factor  $R_{AA}$ . The numerical result, as a function of participant number,  $N_{\text{part}}$ , is compared to the midrapidity RHIC data in Fig. 1. Plots (a) and (b) correspond to the pQCD and thermal charm quark distributions, respectively. The bands are theoretical results including the uncertainty in the initial charm quark and  $\Psi$  production cross sections  $\sigma_{pp}^{c\bar{c}}$  and  $\sigma_{pp}^\Psi$ . The solid and dot-dashed curves indicate calculations with only initial production (without regeneration,  $\beta_\Psi = 0$ ) and only regeneration (without initial production,  $\sigma_{\text{abs}} = \infty$ ). Almost all the initial 40% of  $J/\psi$ s from  $\chi_c$  decay is lost in semicentral collisions [30]. In central collisions, only the directly pro-

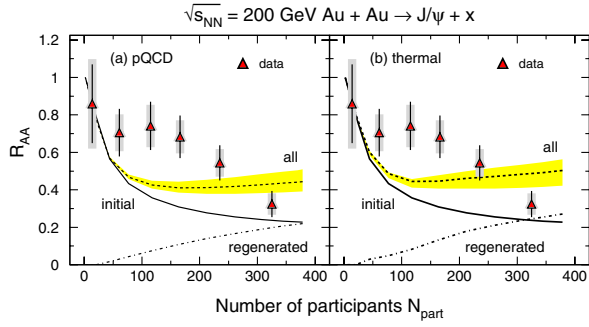


FIG. 1 (color online). The nuclear modification factor  $R_{AA}$  as a function of participant number  $N_{\text{part}}$  in pQCD (a) and thermal (b) charm quark distributions. The solid and dot-dashed curves are the calculations with only initial production and only regeneration. The bands are the full result, including the uncertainty in initial charm quark and  $\Psi$  production. The data are from PHENIX [31].

duced  $J/\psi$ s suffer anomalous suppression. When nuclear absorption effect is reduced by decreasing the initial time  $\tau_0$  or the absorption cross section  $\sigma_{\text{abs}}$ , the initial  $J/\psi$  yield is less suppressed. Because of the strong regeneration in central collisions, the full  $J/\psi$  yield is no longer a monotonically decreasing function of centrality. The data seem to show a flat region at  $50 \leq N_{\text{part}} \leq 150$ . This feature cannot be reproduced in the present model calculations.

The momentum spectra are expected to be more sensitive to the production mechanism than the integrated yields. We show the  $J/\psi$  average squared transverse momentum,  $\langle p_t^2 \rangle$ , as a function of centrality in Fig. 2. It is well known that the multiple gluon scattering in the initial state leads to transverse momentum broadening. The leakage effect due to the anomalous suppression also results in  $p_t$  broadening in central collisions [15]. These two broadening effects on the initial  $J/\psi$ s are reflected in the solid curves in Fig. 2. For the regenerated  $J/\psi$ s, the charm quarks in the pQCD scenario have no scattering in the initial state and in the QGP, and they satisfy the statistic distribution in the thermal scenario. The  $\langle p_t^2 \rangle$  of the regen-

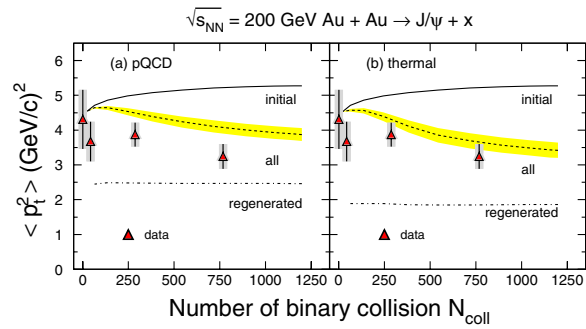


FIG. 2 (color online). The  $J/\psi$  averaged transverse momentum square as a function of the number of binary collision,  $N_{\text{coll}}$ . The calculations are the same as in Fig. 1. The PHENIX [31] data are shown.

erated  $J/\psi$ s in these two limits looks independent of centrality; see the dot-dashed curves in Fig. 2. Since the high momentum charm quarks lose energy during thermalization, the average squared momentum ( $\sim 2 \text{ GeV}^2$ ) in the thermal scenario is smaller than the one ( $\sim 2.5 \text{ GeV}^2$ ) in the pQCD scenario. The collective flow develops with time, the  $\langle p_t^2 \rangle$  for the sudden-produced  $J/\psi$ s on the hadronization hypersurface [19,20,22,23] of QGP is larger than our result for continuously regenerated  $J/\psi$ s in the whole volume of QGP. Because the initial production decreases with centrality, due to absorption and anomalous suppression, and regeneration increases with centrality, shown in Fig. 1, the  $\langle p_t^2 \rangle$  starts at the initial result and approaches the regeneration result as centrality increases.

The  $J/\psi$  elliptic flow,  $v_2$ , is a useful tool for studying charm production mechanism in nuclear collisions. When no regeneration is considered, the leakage effect gives the lower limit of  $J/\psi$   $v_2$  [16], the solid curve in Fig. 3. In the pQCD scenario, charm quarks do not interact with the medium and the regenerated  $J/\psi$ s do not carry any collective property of the system, so we only discuss  $v_2$  in the thermal scenario. If the regeneration occurs only at hadronization of the QGP, the well-developed azimuthal anisotropic flow leads to a large  $J/\psi$   $v_2$ , see discussions in Ref. [22]. However, for the continuous regeneration in the QGP volume the average elliptic flow becomes much smaller since the asymmetric flow is very small in the early stage. At impact parameter  $b = 7.8 \text{ fm}$ , the continuously regenerated  $J/\psi$   $v_2$ , the dot-dashed line in Fig. 3, is only one half of the suddenly regenerated  $J/\psi$   $v_2$  in the coalescence model [22]. To check the difference between the continuous and sudden regeneration mechanisms, we force the regeneration to occur in a thin spherical shell by adjusting the regeneration temperature region to  $T_c \leq T \leq T_c + \delta T$ . Indeed, the regenerated  $v_2$  approaches the value of Ref. [22] for  $\delta T \rightarrow 0$ . Since the  $J/\psi$  yield in semicentral collisions is still dominated by the initial production (see Fig. 1), there is no sizable difference in  $v_2$  between the total (dashed line) and initially produced  $J/\psi$ s (solid line); see Fig. 3.

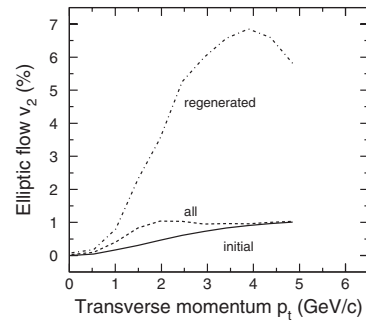


FIG. 3. The  $J/\psi$  elliptic flow in  $\sqrt{s_{NN}} = 200 \text{ GeV}$  Au + Au collisions at impact parameter  $b = 7.8 \text{ fm}$ . The calculations are the same as in Fig. 1.

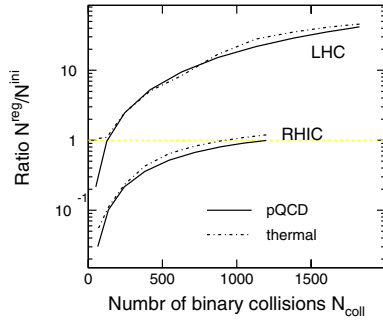


FIG. 4 (color online). The ratio of regenerated to initially produced  $J/\psi$  yields at RHIC and LHC energies in pQCD and thermal scenarios. At the LHC, we choose  $\sigma_{pp}^{\Psi} = 18.9 \mu\text{b}$  [32],  $\sigma_{pp}^{\bar{c}} = 5740 \mu\text{b}$  [33],  $\tau_0 = 0.3 \text{ fm}$ , and initial temperature 680 MeV.

What is the case for nuclear collisions at the LHC? Because of the extremely high center-of-mass energy, the QGP formed at LHC energy will have much higher temperatures, longer lifetimes and larger sizes. Most of the initial  $J/\psi$ s will be suppressed by stronger gluon dissociation in QGP. On the other hand, more charmonia will be created by the regeneration. The ratio  $N^{\text{reg}}/N^{\text{ini}}$  of regenerated to initially produced  $J/\psi$ s is shown as a function of centrality in Fig. 4. While at RHIC, the ratio can reach unity only in the most central collisions, it is much larger than 1 at almost any centrality bin at the LHC. Therefore, regeneration will dominate the observed  $J/\psi$ . As a consequence, the  $J/\psi$   $R_{AA}$ ,  $v_2$ , and  $\langle p_T^2 \rangle$  at the LHC will follow the regeneration calculations in Figs. 1–3.

In summary, by constructing and solving the transport equation for charmoniums together with hydrodynamic evolution of the QGP, we presented a self-consistent way to calculate the  $J/\psi$  transverse momentum distributions. Unlike the cases at the SPS, where initial production is almost the only  $J/\psi$  source and at the LHC, where the regeneration dominates the observed  $J/\psi$ s, both initial production and regeneration are important at RHIC. The average squared transverse momentum with thermalized charm quarks fits the RHIC data reasonably well. In contrast to previous calculations [22] with only sudden regeneration at hadronization, the dominant initial production in semicentral collisions and the continuous regeneration in the whole QGP volume lead to a rather small  $J/\psi$  elliptic flow at RHIC.

We are grateful to R. Rapp and X. Zhu for the helpful discussions. We thank Dr. R. Vogt and Dr. B. Mohanty for proofreading the manuscript. P.Z. thanks A. Kostyuk and H. Stöcker for the useful discussions and the Frankfurt Institute for Advanced Studies for its financial support in the beginning of the work. The work is supported in part by the Chinese Grants No. NSFC10575058, No. 10425810, No. 10435080 and U.S. DOE Contract No. DE-AC03-76SF00098.

- [1] B. Müller and D. K. Srivastava, nucl-th/0407010.
- [2] M. Gyulassy, I. Vitev, X. N. Wang, and B. Zhang, in *Quark Gluon Plasma 3* (World Scientific, Singapore, 2004), p. 123, and references therein.
- [3] J. Adams *et al.* (STAR Collaboration), Nucl. Phys. **A757**, 102 (2005).
- [4] K. Adcox *et al.* (PHENIX Collaboration), Nucl. Phys. **A757**, 184 (2005).
- [5] B. Müller, nucl-th/0404015.
- [6] J. Adams *et al.* (STAR Collaboration), Phys. Rev. Lett. **94**, 062301 (2005); Y. F. Zhang, nucl-ex/0607011.
- [7] S. S. Adler *et al.* (PHENIX Collaboration), Phys. Rev. Lett. **96**, 032301 (2006); **96** 032001 (2006); **94**, 082301 (2005).
- [8] F. Karsch, Eur. Phys. J. C **43**, 35 (2005).
- [9] M. Asakawa and T. Hatsuda, Phys. Rev. Lett. **92**, 012001 (2004).
- [10] T. Matsui and H. Satz, Phys. Lett. B **178**, 416 (1986).
- [11] J.-P. Blaizot and J.-Y. Ollitrault, Phys. Rev. Lett. **77**, 1703 (1996).
- [12] A. Polleri, T. Renk, R. Schneider, and W. Weise, Phys. Rev. C **70**, 044906 (2004).
- [13] A. Capella, A. Kaidalov, A. Kouider Akil, and C. Gerschel, Phys. Lett. B **393**, 431 (1997).
- [14] E. Bratkovskaya, W. Cassing, H. Stöcker, and N. Xu, Phys. Rev. C **71**, 044901 (2005).
- [15] J. Hüfner and P. Zhuang, Phys. Lett. B **559**, 193 (2003).
- [16] X. Zhu, P. Zhuang, and N. Xu, Phys. Lett. B **607**, 107 (2005).
- [17] M. C. Abreu *et al.* (NA50 Collaboration), Nucl. Phys. **A610**, 404c (1996).
- [18] R. V. Gavai *et al.*, Int. J. Mod. Phys. A **10**, 3043 (1995).
- [19] P. Braun-Munzinger and J. Stachel, Phys. Lett. B **490**, 196 (2000); Nucl. Phys. **A690**, 119c (2001).
- [20] M. I. Gorenstein, A. P. Kostyuk, H. Stöcker, and W. Greiner, Phys. Lett. B **509**, 277 (2001).
- [21] L. Grandchamp and R. Rapp, Phys. Lett. B **523**, 60 (2001); Nucl. Phys. **A709**, 415 (2002).
- [22] V. Greco, C. M. Ko, and R. Rapp, Phys. Lett. B **595**, 202 (2004).
- [23] L. Grandchamp, R. Rapp, and G. E. Brown, Phys. Rev. Lett. **92**, 212301 (2004).
- [24] R. L. Thews and M. L. Mangano, Phys. Rev. C **73**, 014904 (2006).
- [25] A. Zoccoli *et al.* (HERA-B Collaboration), Eur. Phys. J. C **43**, 179 (2005).
- [26] S. S. Adler *et al.* (PHENIX Collaboration), Phys. Rev. Lett. **96**, 012304 (2006).
- [27] R. Vogt, Phys. Rev. C **71**, 054902 (2005).
- [28] M. E. Peskin, Nucl. Phys. **B156**, 365 (1979); G. Bhanot and M. E. Peskin, Nucl. Phys. **B156**, 391 (1979).
- [29] S. S. Adler *et al.* (PHENIX Collaboration), Phys. Rev. Lett. **94**, 082301 (2005).
- [30] F. Karsch, D. Kharzeev, and H. Satz, Phys. Lett. B **637**, 75 (2006).
- [31] H. Pereira Da Costa *et al.* (PHENIX Collaboration), Nucl. Phys. **A774**, 747 (2006).
- [32] M. Bedjidian *et al.*, hep-ph/0311048.
- [33] R. Vogt, Int. J. Mod. Phys. E **12**, 211 (2003).